Part V

Foundation

Foundation Analysis

Chapter 1 Soil Response Curves under Horizontal Loads

Chapter 2 Soil Response Curve for Axial Load

Chapter 3 Effects on Group Piles under Lateral Loads

Foundation

Foundation Analysis / 001

Chapter 1 **Soil Response Curves under Horizontal Loads / 003**

1.1 Soft Cohesive Soil under Free Surface / 005
1.2 Stiff Cohesive Soil under Free Surface / 009
1.3 Stiff Cohesive Soil Unaffected by Free Surface / 015
1.4 Sandy Soil under Groundwater Table / 018
1.5 Soil Response Curve for Sandy Soil / 024
1.6 Soil Response Curve for $c-\phi$ Soil / 027
1.7 Ground Response Curve for Rock / 033
1.7.1 Soil Response Curve for Hard Rock / 033
1.7.2 Ground Response Curve for Weak Rock / 034

Chapter 2 **Soil Response Curve for Axial Load / 038**

2.1 Overview / 038
2.2 Load Transfer Curve for Frictional Resistance in Cohesive Soil / 041
2.3 Load Transfer Curve at Pile Tip in Cohesive Soil / 043
2.4 Load Transfer Curve for Frictional Resistance in Sandy Soil / 045
2.5 Load Transfer Curve at Pile Tip in Sandy Soil / 047

Chapter 3 **Effects on Group Piles under Lateral Loads / 049**

3.1 Overview / 049

3.2 Reduction Factors for Loading in Transverse Direction / 051

3.3 Reduction Factors for Loading in Longitudinal Direction / 052

3.4 Reduction Factors for Diagonal Group Piles / 054

Foundation Analysis

Foundation analysis, which has been mainly performed for vertical loads on structures, recently has been extended to the analysis of piles subjected to horizontal loads such as wind loads, wave loads, etc. For this type of analysis, analytical models that can reflect the nonlinear behaviors of soils have become necessary. Reese and Matlock et al. conducted lateral load tests for various types of soils and proposed soil response curves, which compiled the magnitudes of subgrade reactions at various depths relative to pile deflections beyond the elastic limits until yielding of the soils. When lateral loads act on a pile head, especially in case of soft soil, the soil stress easily exceeds the elastic limit even under small external loads. In such cases, nonlinear soil response curves need to be used; otherwise, a wide difference between the actual behavior and the analytical behavior is expected.

The elements, loads and boundary conditions used in Foundation Analysis of SoilWorks are listed in Table (1) (refer to Part II Tunnel for further details).

Table 1 Elements, loads and boundary conditions used in foundation analysis

Main category	Sub-category	Application
Element	Soil element	Nonlinear Point Spring
	Pile element	Beam
	Foundation element	Rigid Link
Load	Load acting on pile head	Nodal load
Boundary	Pile head boundary	Beam end release
	Pile tip boundary	Support boundary

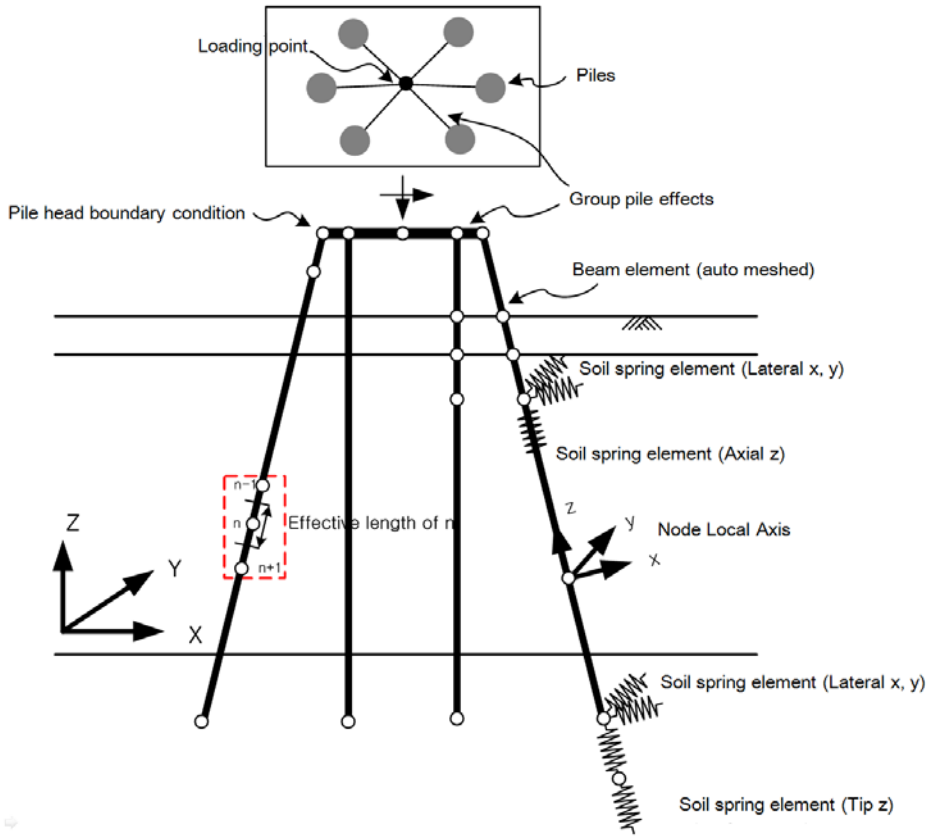

Figure 1 Structural system for foundation analysis

Chapter 1

Soil Response Curves under Horizontal Loads

When a horizontal load is applied to a pile, the pile exhibits a nonlinear resistance (p) – displacement (y) behavior. Figure 1.1 presents the concept of a soil response curve proposed by Reese (1983). After a pile is placed, a uniform stress appears in every direction at a depth of x_1. However, once the pile undergoes displacement, the stress increases at the front of the pile and decreases at the back of the pile.

If the soil reaction (p) can be defined as a function of depth below the ground surface (x) and pile displacement (y), the pile behavior can be analyzed using the soil response curve. The pile behavior can be approximately analyzed by calculating the ultimate soil resistance (p_u) at each depth.

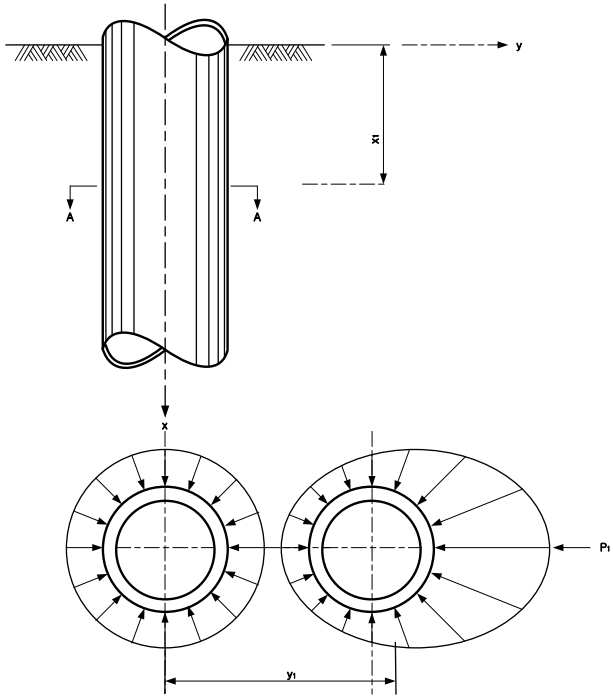

Figure 1.1 Definition of soil response curve

As shown in Figure 1.2 for a pile subjected to a horizontal load, the soil modulus of deformation (E_s) exhibits the maximum stiffness under a small displacement and a decrease in the stiffness as the displacement increases, which resembles a spring behavior. The dotted line signifies the soil stiffness, and the slope becomes gentle as the deformation progresses. In general, the shear strength increases with depth, which causes the soil modulus of deformation to increase as shown in Figure 1.2b.

As the slope varies, nonlinear material properties are incorporated into the p-y curve to better coincide with the true behavior. A process of iterative analysis is thus required to attain convergence.

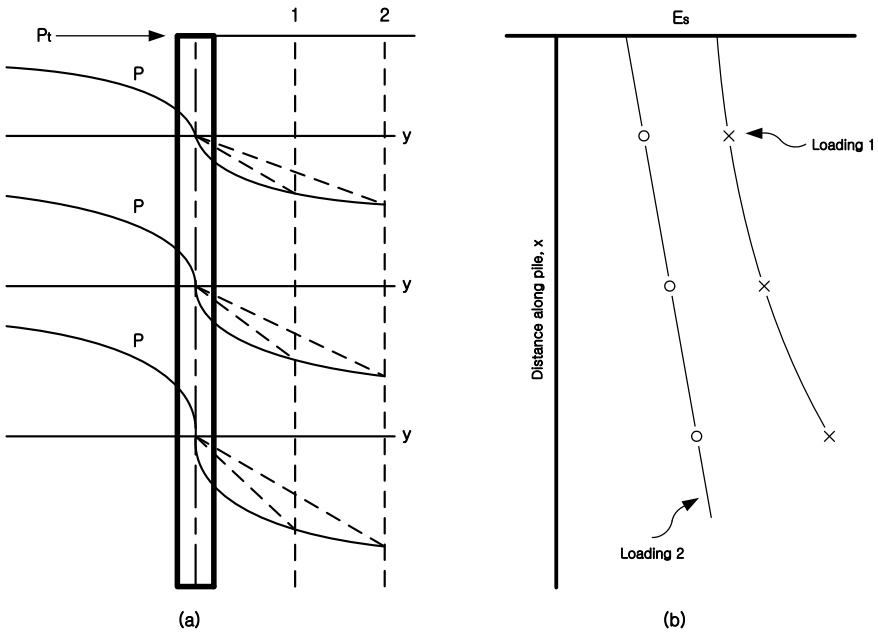

Figure 1.2 Soil response curves by depths

The three factors that affect a p-y curve the most are soil types, pile dimensions and the characteristics of loads.

1.1 Soft Cohesive Soil under Free Surface

Matlock (1970) conducted lateral load tests on a steel pipe pile with a diameter of $12.75\,ft$ and a length of $42\,ft$ and presented p-y curves for soft cohesive soil. The p-y curves were based on the in-situ load tests of shear strength of $800 lb/ft^2$ (Lake Austin) and the average shear strength of $300 lb/ft^2$ (Sabine Pass, Texas).

The figures below show the soil response curves for soft cohesive soil under short term static loading. The load tests were conducted not only for static loading, but also for cyclic loading. In case of cyclic loading, groundwater had a great influence on the responses.

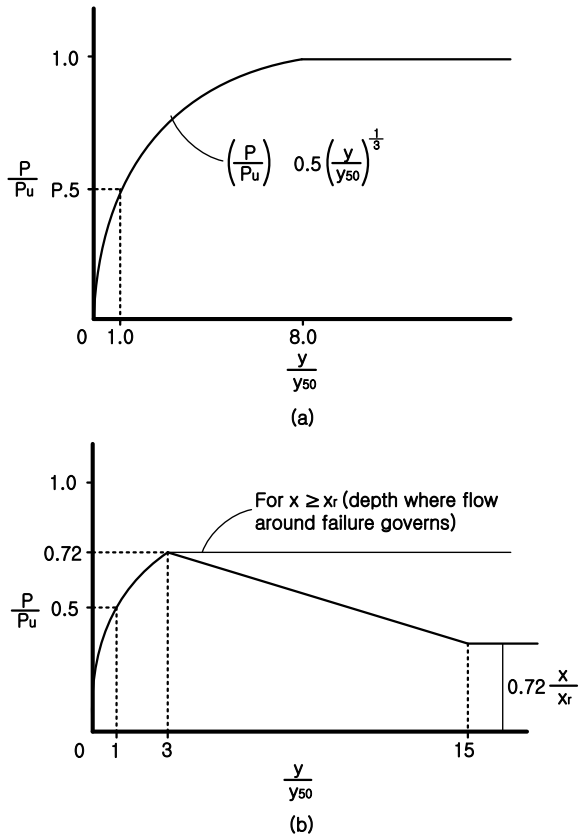

Figure 1.1.1 Soil response curves in soft cohesive soil below a free surface

The soil response curve in soft cohesive soil under the action of static loading is determined by the following procedures:

① Measure the undrained shear strength (c_u) and saturated unit weight (γ) at each corresponding depth of soil. And determine ε_{50}, which is the strain corresponding to 50% of the maximum deviator stress. If the stress-strain curve is unavailable, obtain a general value of ε_{50} from Table (1.1.1).

Table 1.1.1 Strain values of cohesive soil

Consistency of cohesive soil	ε_{50}
Soft	0.020
Medium	0.010
Stiff	0.005

② Determine the ultimate subgrade reaction per unit length of a pile. Use the lesser of the following two expressions to determine the ultimate subgrade reaction, p_u:

$$p_u = \left(3 + \frac{\gamma'}{c}x + \frac{J}{b}x\right)cb \qquad (1.1.1)$$

$$p_u = 9cb \qquad (1.1.2)$$

γ' above is the average effective unit weight from the ground surface to the corresponding depth, x; c is the shear strength at the depth of x; b is the pile width; and J is 0.5 for soft clay and 0.25 for medium stiff clay according to the tests conducted by Matlock (1970). Since 0.5 for J is generally used, Soilworks also has adopted the value 0.5.

③ Determine y_{50}, which is the displacement corresponding to 50% of the ultimate subgrade reaction from the following equation:

$$y_{50} = 2.5\varepsilon_{50}b \qquad (1.1.3)$$

④ Determine the p-y curve from the following equation:

$$\frac{p}{p_u} = 0.5\left(\frac{y}{y_{50}}\right)^{\frac{1}{3}} \tag{1.1.4}$$

⑤ When $y \geq 8y_{50}$ as shown in Figure 1.1.1, $p = p_u$ is maintained.

Under the action of cyclic loading, the soil response curve in soft cohesive soil is determined by the following procedures:

⑥ When $p \leq 0.72p_u$, determine the p-y curve in the same way as was done for static loading.

⑦ By solving the simultaneous equations (1.1.1) and (1.1.2), the transition point x_r at which two p_u s become equal can be found. If the shear strength and the unit weight are constantly maintained, the transition point is calculated by Eq. (1.1.5). However, if the shear strength and the unit weight vary with depth, the transition point x_r must be calculated according to the soil properties.

$$x_r = \frac{6cb}{(\gamma' b + Jc)} \tag{1.1.5}$$

⑧ If the point x at which the p-y curve is determined is deeper than the transition point x_r, p becomes equal to p_u at the point $y \geq 3y_{50}$.

⑨ If the point x at which the p-y curve is determined is shallower than the transition point x_r, $p = 0.72p_u$ at the point $y = 3y_{50}$. The subgrade reaction decreases with the increase in displacement, and p is given by Eq. (1.1.6) until the point $y = 15y_{50}$.

$$p = 0.72p_u\left(\frac{x}{x_r}\right) \tag{1.1.6}$$

⑩ When $y \geq 15y_{50}$, p remains constant.

Recommended Soil Tests

Matlock (1970) recommended the following tests in order to determine the shear strength of

soil, which is an important parameter in determining the p-y curve:

① Specimen sampling and in-situ vane shear test for soil classification

② Unconsolidated and undrained triaxial compression test under the same confining pressure as the overburden load

③ Scaled down vane test of specimen

④ Unconfined compression test

The above tests must be conducted in order to determine the unit weight of soil.

1.2 Stiff Cohesive Soil under Free Surface

Reese, Cox and Koop (1975) conducted lateral load tests in stiff cohesive soil on a steel pipe pile with a diameter of $24in$ and a length of $50\,ft$. The undrained shear strength of the cohesive soil varied from $1ton/ft^2$ at the ground surface to $3ton/ft^2$ at the depth of $12\,ft$.

Figure 1.2.1 illustrates the test results under short term static loading. Soil tests for cyclic loading were also conducted at the same site. The results of the tests showed that the soil resistance against the cyclic loading was considerably lower than that against the static loading even though the tests were carried out at the same location. Long and Reese (1983) could not identify the cause of the findings but only concluded that the p-y curves presented by the load tests were very conservative.

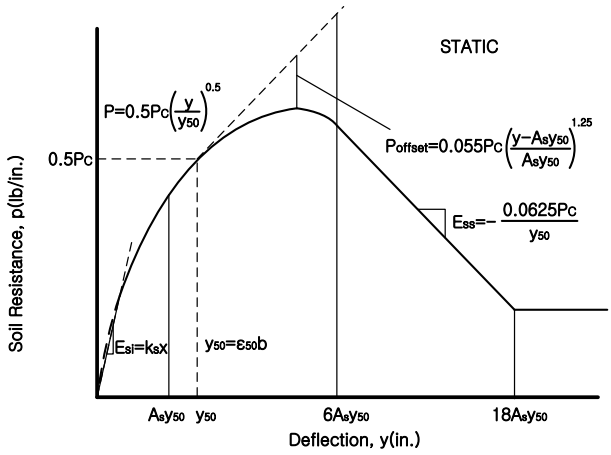

Figure 1.2.1 Soil response curve in stiff cohesive soil below a free surface under static loading

The soil response curve in stiff cohesive soil under the action of static loading is determined by the following procedures:

① Measure the undrained shear strength (c_u), saturated unit weight (γ') and pile diameter (b) at each corresponding depth.

② Calculate the average undrained shear strength, c_a up to the depth of x.

③ Determine the ultimate subgrade reaction per unit length of a pile. Use the lesser of the following two expressions to determine the ultimate subgrade reaction:

$$p_{ct} = 2c_a b + \gamma' bx + 2.83 c_a x \quad (1.2.1)$$

$$p_{cd} = 11cb \quad (1.2.2)$$

④ Determine the non-dimensional depth coefficient, ($A_s = \frac{x}{b}$) from Figure 1.2.2.

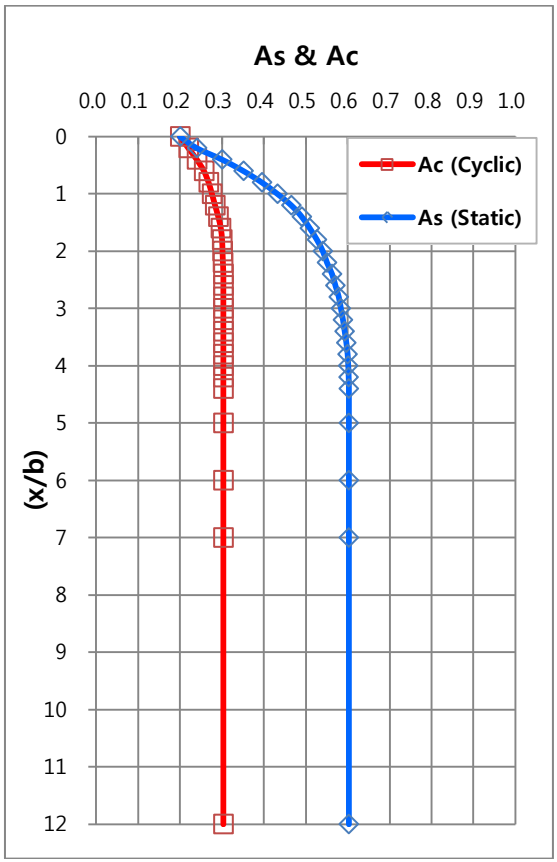

Figure 1.2.2 Coefficients As and Ac

⑤ The initial straight line portion of the p-y curve is given by,

$$p = (kx)y \tag{1.2.3}$$

where k values (k_s and k_c) are defined in Table (1.2.1).

Table 1.2.1 Modulus of subgrade reaction based on average undrained shear strength

	Average undrained shear strength ($tonf / ft^2$)		
	0.5-1	1-2	2-4
k_s (static loading, lb / in^3)	500	1000	2000
k_c (dynamic loading, lb / in^3)	200	400	800

⑥ y_{50} is given by,

$$y_{50} = \varepsilon_{50} b \tag{1.2.4}$$

ε_{50} is determined by tests. In the absence of tests, determine the value from Table (1.2.2).

Table 1.2.2 Strain based on average undrained shear strength

	Average undrained shear strength ($tonf / ft^2$)		
	0.5-1	1-2	2-4
ε_{50}	0.007	0.005	0.004

⑦ The initial curve part of the p-y curve can be determined from Eq. (1.2.5), where p_c is calculated from Eq. (1.2.1) and Eq. (1.2.2).

$$p = 0.5 p_c \left(\frac{y}{y_{50}} \right)^{0.5} \tag{1.2.5}$$

Eq. (1.2.5) is valid from the point where Eq. (1.2.5) and Eq. (1.2.3) intersect to $y = A_s y_{50}$.

⑧ The second curve part of the p-y curve is calculated from Eq. (1.2.6).

$$p = 0.5 p_c \left(\frac{y}{y_{50}} \right)^{0.5} - 0.055 p_c \left(\frac{y - A_s y_{50}}{A_s y_{50}} \right)^{1.25} \tag{1.2.6}$$

Eq. (1.2.6) is valid from $y = A_s y_{50}$ to $y = 6 A_s y_{50}$.

⑨ The next part is a straight line and is given by,

$$p = 0.5 p_c \left(6 A_s \right)^{0.5} - 0.411 p_c - \left(\frac{0.0625}{y_{50}} \right) p_c \left(y - 6 A_s y_{50} \right) \tag{1.2.7}$$

Eq. (1.2.7) is valid from $y = 6 A_s y_{50}$ to $y = 18 A_s y_{50}$.

⑩ The last straight line part is expressed by,

$$p = 0.5 p_c \left(6 A_s \right)^{0.5} - 0.411 p_c - 0.75 p_c A_s \tag{1.2.8}$$

$$p = p_c \left(1.225 \sqrt{A_s} - 0.75 A_s - 0.411 \right) \tag{1.2.9}$$

Eq. (1.2.8) is valid for $y \geq 18 A_s y_{50}$.

In the process of completing the soil response curve by parts, if a point where Eq. (1.2.3) and Eq. (1.2.5) intersect exists, the p-y curve is defined as shown in Figure 1.2.3. However, if Eq. (1.2.3) does not intersect with other equations, Eq. (1.2.3) is extended to a point where Eq. (1.2.3) intersects with the next curve. If no intersection point exists at all, Eq. (1.2.3) alone defines the p-y curve.

The p-y curve under the action of cyclic loading is defined by the following procedures:

Repeat the procedures ①, ②, ③, ⑤ and ⑥ in the same way as was done for static loading.

④ Determine the cyclic loading coefficient A_c corresponding to the non-dimensional

depth $\frac{x}{b}$ from Figure 1.2.2.

$$y_p = 4.1 A_c y_{50} \tag{1.2.10}$$

⑦ The curve part of the p-y curve is given by,

$$p = A_c p_c \left[1 - \left| \frac{y - 0.45 y_p}{0.45 y_p} \right|^{0.25} \right] \tag{1.2.11}$$

Eq. (1.2.11) is valid from the point where Eq. (1.2.11) and Eq. (1.2.3) intersect to $y = 0.6 y_p$.

⑧ The next straight line part of the p-y curve is defined as follows:

$$p = 0.936 A_c p_c - \frac{0.085}{y_{50}} p_c \left(y - 0.6 y_p \right) \tag{1.2.12}$$

Eq. (1.2.12) is valid from $y = 0.6 y_p$ to $y = 1.8 y_p$.

⑨ The last straight line part is defined as follows:

$$p = 0.936 A_c p_c - \frac{0.102}{y_{50}} p_c y_p \tag{1.2.13}$$

Eq. (1.2.13) is valid for the range of $y = 1.8 y_p$.

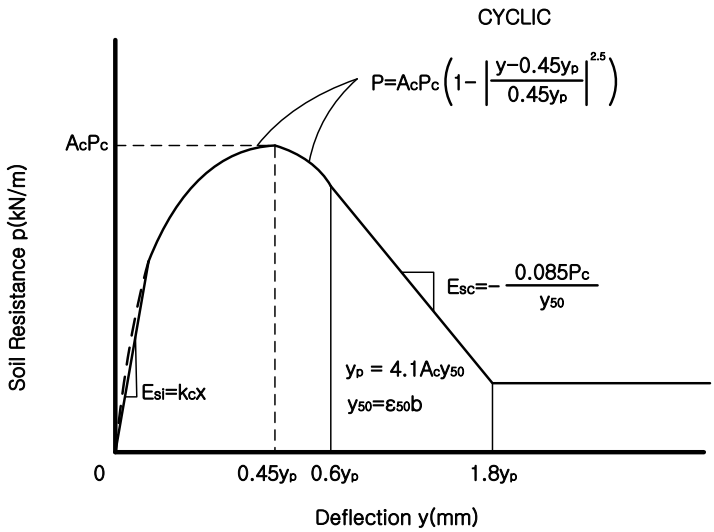

Figure 1.2.3 Soil response curve in stiff cohesive soil below a free surface under cyclic loading

Even under the condition of cyclic loading, if there is a point where Eq. (1.2.3) and Eq. (1.2.11) intersect, the curve as shown in Figure 1.2.3 is generated. However, if no intersection exists between Eq. (1.2.3) and other equations, the smaller value is used.

Recommended Soil Tests

The following tests are recommended to obtain the p-y curve in stiff cohesive soil:
① Measure the shear strength of soil through unconsolidated and undrained triaxial compression in-situ tests under confining pressure.

② The strain, ε_{50} corresponding to 50% of the maximum deviator stress can be determined through laboratory tests using undisturbed specimens.

③ Triaxial compression tests are recommended to determine the shear strength of stiff cohesive soil. Although the shear strength estimated by triaxial compression tests is somewhat conservative, such tests present the most realistic strength level compared to other tests concerning the pile behavior analysis. Unit weight assessment needs to be also conducted.

1.3 Stiff Cohesive Soil Unaffected by Free Surface

Welch and Reese (1972, 1975) conducted in-situ load tests and proposed the soil response curve for stiff cohesive soil unaffected by a free surface. The pile used in the load tests is $36in$ in diameter with the buried length of $42\,ft$. The average undrained shear strength of the cohesive soil used was $2,200lb/ft^2$ measured at the depth of $20\,ft$ from the ground surface.

Figure 1.3.1 illustrates the pile behavior under the action of short term static loading. The curve is defined by the following procedures:

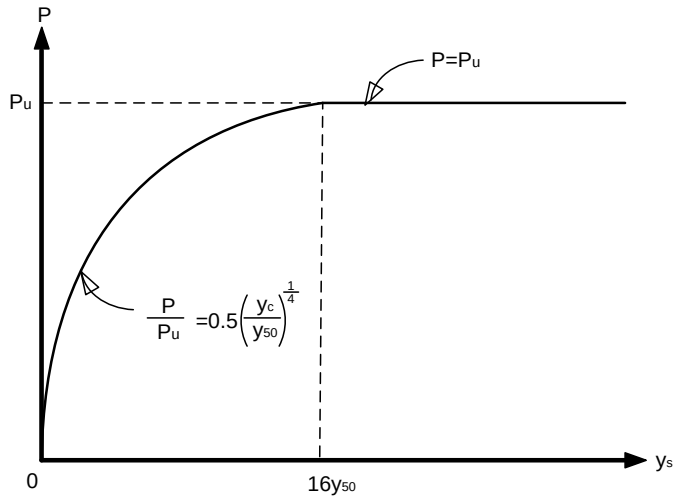

Figure 1.3.1 Soil response curve for stiff clay unaffected by a free surface under static loading

① Determine the undrained shear strength (c_u), unit weight (γ) and pile diameter (b) at each corresponding depth. And determine ε_{50} from the stress-strain curve. If the stress-strain curve is unavailable, use Table 1.1.1. In general, a value between 0.01 and 0.005 is used. The larger the value, the more stable results can be obtained.

② Determine the ultimate subgrade reaction per unit length of a pile. Calculate the

ultimate subgrade reaction, p_u in the same way as was done for soft cohesive soil. Use the lesser of Eq. (1.1.1) and Eq. (1.1.2).

③ Determine the displacement corresponding to 50% of the ultimate subgrade reaction, y_{50} from Eq. (1.1.3).

④ The initial part of the p-y curve is given by,

$$\frac{p}{p_u} = 0.5\left(\frac{y}{y_{50}}\right)^{0.25} \tag{1.3.1}$$

⑤ $p = p_u$ is constantly maintained when $y \geq 16 y_{50}$.

The behavior under the action of cyclic loading is presented in Figure 1.3.2, and the procedures are as follows:

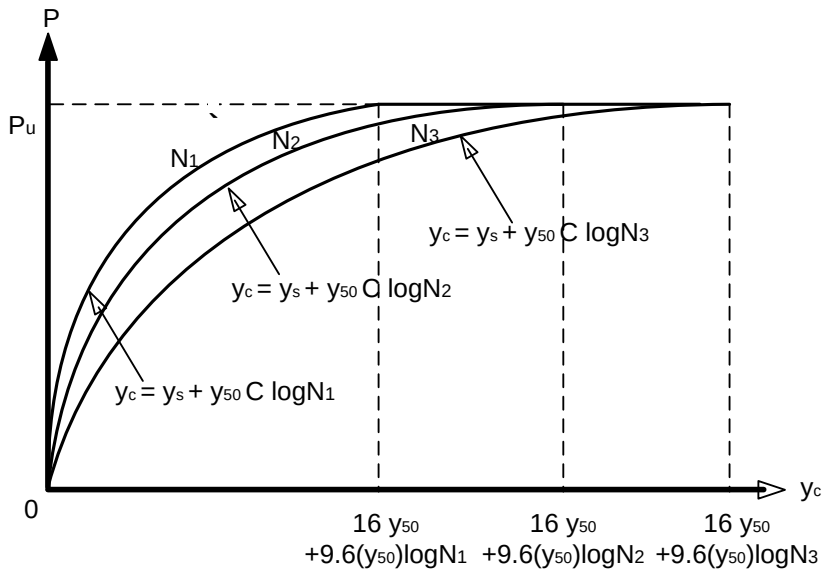

Figure 1.3.2 Soil response curve for stiff clay unaffected by a free surface under cyclic loading

① Determine the p-y curve in the same way as was done for static loading.

② Determine the number of load cycles through which cyclic loading is applied to a pile.

③ The cyclic loading influence factor, C is determined by laboratory cyclic load tests. The value of $\frac{p}{p_u}$, which depends on soil types and the increase in the number of loading cycles, is calculated, and the trend in changes is calculated by the equation. In the absence of such data, Eq. (1.3.2) proposed by Welch and Reese (1972) is used.

$$C = 9.6\left(\frac{p}{p_u}\right)^4 \tag{1.3.2}$$

④ Using C calculated above, y_c is determined as follows:

$$y_c = y_s + y_{50} \cdot C \cdot \log N \tag{1.3.3}$$

y_c above is the displacement due to the N th cyclic load; y_s is the displacement due to short term static loading; y_{50} is the displacement at 50% of the ultimate resistance due to short term static loading; and N is the number of loading cycles.

⑤ In case of cyclic loading, the p-y curve for the number of cycles (N) is defined using y_c in lieu of y_s .

Recommended Soil Tests

By conducting undrained triaxial compression tests, the shear strength of cohesive soil and the stress-strain curve can be obtained. In general, in-situ strength tests for cohesive soil are conducted to evaluate the shear strength of soil, and laboratory tests on undisturbed specimens are conducted to obtain the stress-strain curve. The strength parameters obtained from these tests should be properly used depending on the purpose of use and the object of analysis. More test items can be added if necessary. Basically, material tests should be conducted to measure the unit weight of soil.

1.4 Sandy Soil under Groundwater Table

Cox, Reese and Grubbs (1974) conducted lateral load tests in sandy soil using a pile with a diameter of $24in$ and a length of $69\,ft$. The tests were conducted under both static loading and cyclic loading, and the soil responses were measured. The internal friction angle of the sandy soil used was $39°$ and the saturated unit weight was $66lb/ft^3$.

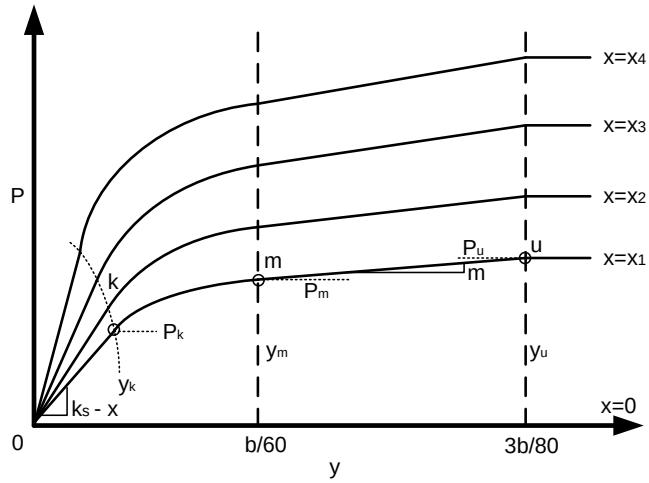

Figure 1.4.1 Soil response curve in sandy soil under both static loading and cyclic loading

The soil response curve under the action of short term static loading is defined as follows:

① Define the internal friction angle (ϕ) and unit weight (γ) of the corresponding sandy soil and the pile diameter (b).

② Determine the following parameters:

$$\alpha = \frac{\phi}{2}$$

$$\beta = 45 + \frac{\phi}{2}$$

$$K_0 = 0.4$$

$$K_a = \tan^2\left(45 - \frac{\phi}{2}\right)$$

③ Calculate the ultimate subgrade reaction of sandy soil per unit length of a pile. Use the lesser of the following two expressions for the ultimate subgrade reaction:

$$p_{st} = \gamma x \left[\frac{K_0 \cdot x \cdot \tan\phi \cdot \sin\beta}{\tan(\beta - \phi) \cdot \cos\alpha} + \frac{\tan\beta}{\tan(\beta - \phi)}(b + x \cdot \tan\beta \cdot \tan\alpha) + K_0 \cdot x \cdot \tan\beta(\tan\phi \sin\beta - \tan\alpha) - K_a b \right] \quad (1.4.1)$$

$$p_{sd} = K_a \cdot b \cdot \gamma \cdot x(\tan^8 - 1) + K_0 \cdot b \cdot \gamma \cdot x \cdot \tan\phi \cdot \tan^4\beta \quad (1.4.2)$$

④ Calculate the intersection point, x_t of Eq. (1.4.1) and Eq. (1.4.2). Use Eq. (1.4.1) for the upper part of the transition point x_t, and use Eq. (1.4.2) for the lower part.

⑤ Determine the corresponding depth, x at which the p-y curve will be calculated.

⑥ Calculate the ultimate subgrade reaction at the point where the ultimate displacement, ($y_u = \frac{3b}{80}$) occurs as follows:

$$p_u = A_s p_s \quad \text{or} \quad p_u = A_c p_s \quad (1.4.3)$$

A_s and A_c above are defined for the non-dimensional depth as shown in Figure 1.4.2 for static loading and cyclic loading respectively. Use a proper p_s which is determined by Eq. (1.4.1) and Eq. (1.4.2) from the step 3.

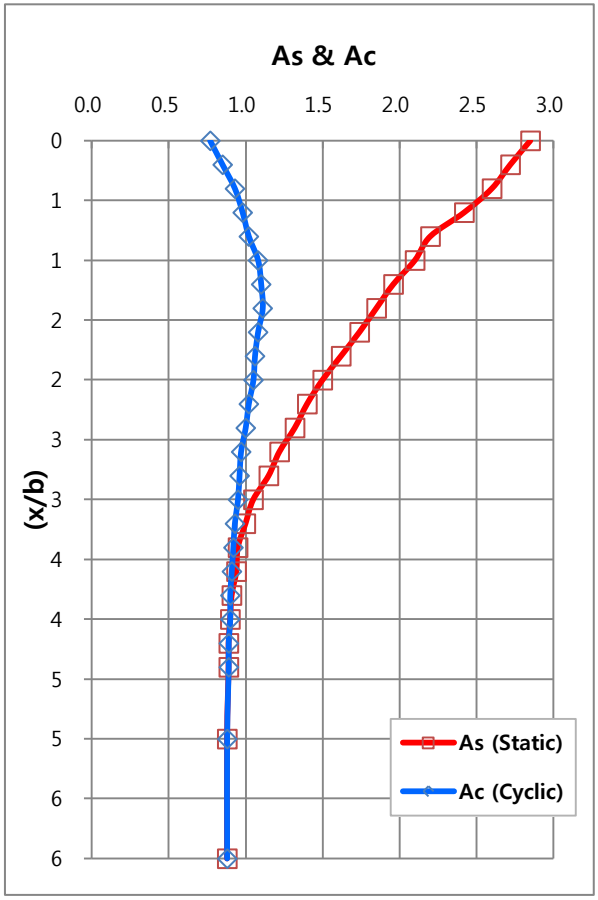

Figure 1.4.2 Constants As and Ac

⑦ Calculate the subgrade reaction, (p_m) corresponding to the pile displacement ($y_m = \frac{b}{60}$) .

$$p_m = B_s p_s \quad \text{or} \quad p_m = B_c p_s \tag{1.4.4}$$

B_s and B_c above are defined for the non-dimensional depth as shown in Figure 1.4.3 for

static loading and cyclic loading respectively. Proper p_s is used. The slope of the soil response curve is m after the displacement reaches $y_m = \frac{b}{60}$ and gradually increases linearly until the curve meets p_u.

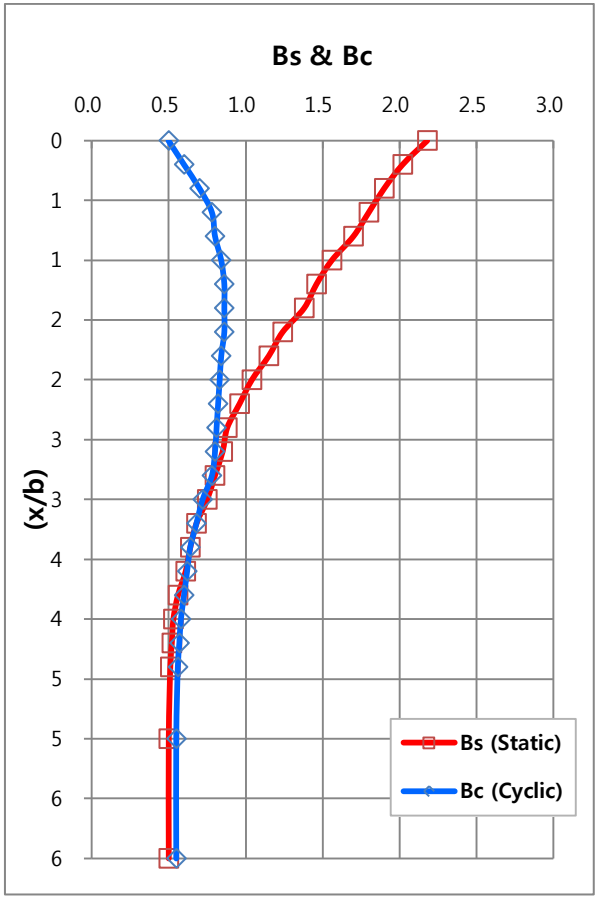

Figure 1.4.3 Constants Bs and Bc

⑧ The initial straight line part of the p-y curve is defined as,

$$p = (kx)\,y \tag{1.4.5}$$

The parameter, k above is obtained from Tables 1.4.1 and 1.4.2.

Table 1.4.1 Typical k values below groundwater level

Relative density	Loose	Medium	Dense
k (lb/in^3)	20	60	125

Table 1.4.2 Typical k values above groundwater level

Relative density	Loose	Medium	Dense
k (lb/in^3)	20	90	225

⑨ The parabolic part of the p-y curve is given by,

$$p = \overline{C} \cdot y^{1/n} \tag{1.4.6}$$

The additional procedures to calculate the parabolic curve between k and m are as follows:

a. The slope between m and u is given by,

$$m = \frac{p_u - p_m}{y_u - y_m} \tag{1.4.7}$$

b. The degree, n of the curve between k and m is given by,

$$n = \frac{p_m}{m \cdot y_m} \tag{1.4.8}$$

c. The coefficient $\overline{C}$ is defined as,

$$\overline{C} = \frac{p_m}{y_m^{1/n}} \tag{1.4.9}$$

d. The location of k is determined by,

$$y_k = \left(\frac{\overline{C}}{k \cdot x} \right)^{\frac{n}{n-1}} \tag{1.4.10}$$

e. Appropriate parameters are defined from the above equations to determine the parabolic part in Eq. (1.4.6).

If an intersection point, k exists between the initial straight line equation and the parabolic equation, the p-y curve is defined as shown in Figure 1.4.1. However, if no intersection point exists between the straight line and the parabola, the p-y curve is completed by finding an intersection point with a subsequent equation. If no intersection point exists with the subsequent equation, the initial straight line equation defines the entire p-y curve.

The soil response curve under cyclic loading is determined in the same way as was done for static loading. But k_c, A_c and B_c are used in lieu of k_s, A_s and B_s.

Recommended Soil Tests

The internal friction angle of soil is determined through conducting triaxial compression tests subjected to the confining pressure due to the effective overburden. However, it is not easy to conduct triaxial compression tests to analyze the pile behavior in sandy soils because it is impossible to sample undisturbed specimens. Therefore, good engineering judgment needs to be exercised depending on the field condition. For sandy soils in general, in-situ tests such as standard penetration test and pressuremeter test are widely used.

1.5 Soil Response Curve for Sandy Soil (API RP2A)

This section describes the soil response curve for sandy soil, which is presented by America Petroleum Institute. The p-y curve for sandy soil presented by API includes empirical factors obtained from the field. In general, no significant difference in the ultimate subgrade reaction (p_u) exists between the ones presented by Reese and API. The equation presented by API is more convenient. The biggest differences are the initial modulus of subgrade reaction and the shape function of the curve.

The p-y curves presented by API RP2A (1987) under the actions of short term static loading and cyclic loading are calculated by the equations below.

① Determine the internal friction angle (ϕ), unit weight (γ) and pile diameter (b).

② Calculate the ultimate subgrade reaction at the corresponding depth, x. Apply Eq. (1.5.1) at shallow depths and Eq. (1.5.2) at deep depths. Use the lesser of the following two expressions:

$$p_{us} = \left(C_1 x + C_2 b\right)\gamma' x \qquad (1.5.1)$$

$$p_{ud} = C_3 b \gamma' x \qquad (1.5.2)$$

p_u above is the ultimate subgrade reaction per unit length; γ' is the effective unit weight; x is the corresponding depth, ϕ is the internal friction angle of sandy soil; C_1, C_2 and C_3 are coefficients defined as a function of the friction angle (ϕ) as shown in Figure 1.5.1; and b is the average pile diameter.

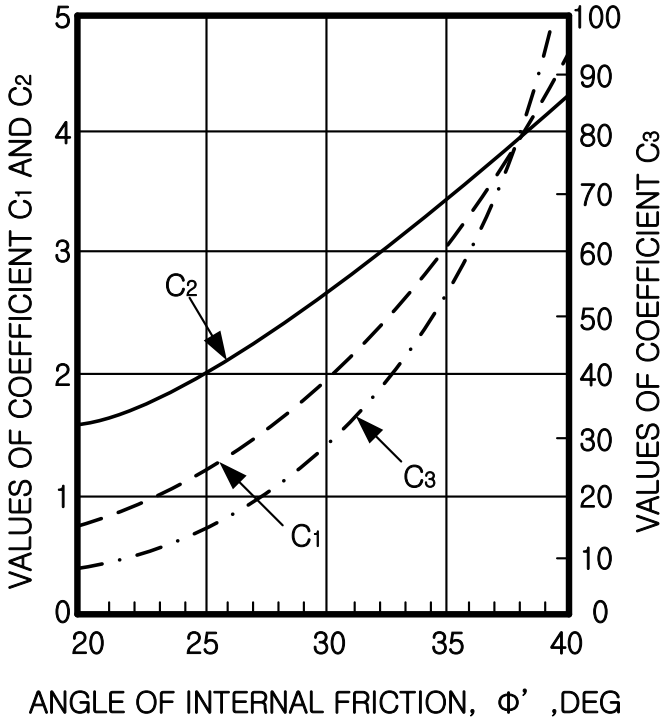

Figure 1.5.1 Coefficients corresponding to friction angles

③ Define the load-displacement curve from p_u calculated at the step ②. The lateral subgrade reaction-displacement relationship for sandy soil is nonlinear, expressed by the equation below.

$$p = Ap_u \tanh\left[\frac{kx}{Ap_u} y\right] \tag{1.5.3}$$

A above is the coefficient calculated under the action of static or cyclic loading.

$A = \left(3.0 - 0.8\frac{x}{b}\right) \geq 0.9$ for static loading,

$A = 0.9$ for cyclic loading

p_u is the lesser of Eq. (1.5.1) and Eq. (1.5.2). k is the initial modulus of subgrade reaction, which is calculated from the function of internal friction angle (ϕ) as shown in Figure 1.5.2. y is the lateral displacement. x is the corresponding depth.

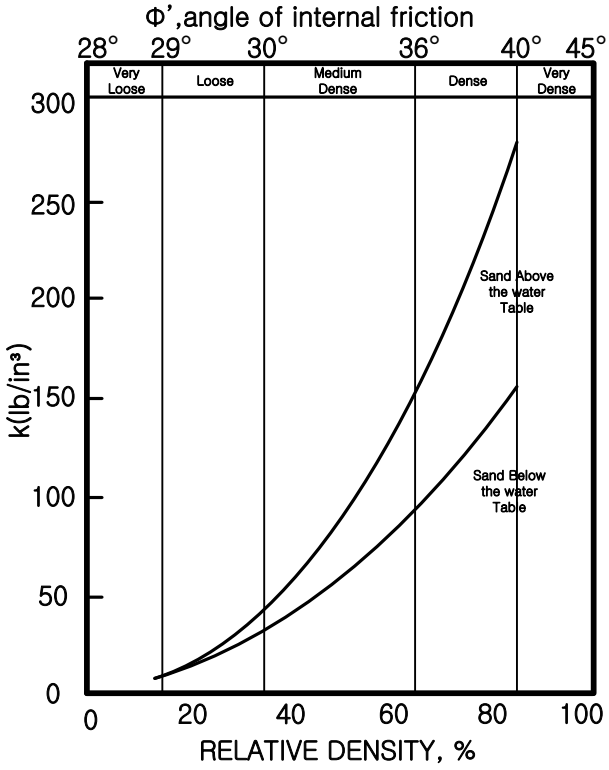

Figure 1.5.2 Initial modulus of subgrade reaction for sandy soil presented by API

1.6 Soil Response Curve for $c-\phi$ Soil

The previous sections described the soil response curves for pure cohesive and pure sandy soils. The reason for limiting the soil types to one type of properties of cohesiveness or internal friction angle was merely out of design convenience and safety. However, most natural soils retain both c and ϕ, rather than being either pure cohesive soil or pure sandy soil.

The failure envelop from strength tests especially for partially saturated cohesive soil shows that the soil retains both c and ϕ simultaneously. When the soil becomes saturated due to a rise in groundwater level or rainfall, it retains pure cohesive soil properties. However, since the pile behavior in unsaturated soil exhibits a state of weakness, it is necessary to define soil response curves reflecting both c and ϕ. Also when sandy soil becomes cemented, the component of cohesion increases leading to an increase in shear strength. Such a phenomenon often occurs in shallow ground layers.

A typical case of the presence of both c and ϕ is consolidated cohesive soil in a drained condition. In other words, when cohesive soil undergoes consolidation for a long period and the groundwater level changes, the soil ends up retaining both cohesion and internal friction angle.

Figure 1.6.1 illustrates the soil response curve under the action of short term static loading or cyclic loading. The procedure is very similar to that for obtaining the soil response curve for sandy soil presented earlier. Conceptually, the ultimate subgrade reaction (p_u) is considered as the passive resistance of soil at the fore side of the pile when the pile moves due to lateral loads. In addition, when the resistance acting on the sides of the pile is added, the total resistance does not exceed the active force exerting on the rear of the pile. Since the active earth pressure acting at the rear of the pile and the resistance developed on the sides of the pile are relatively small compared to the passive resistance, they are ignored in most cases.

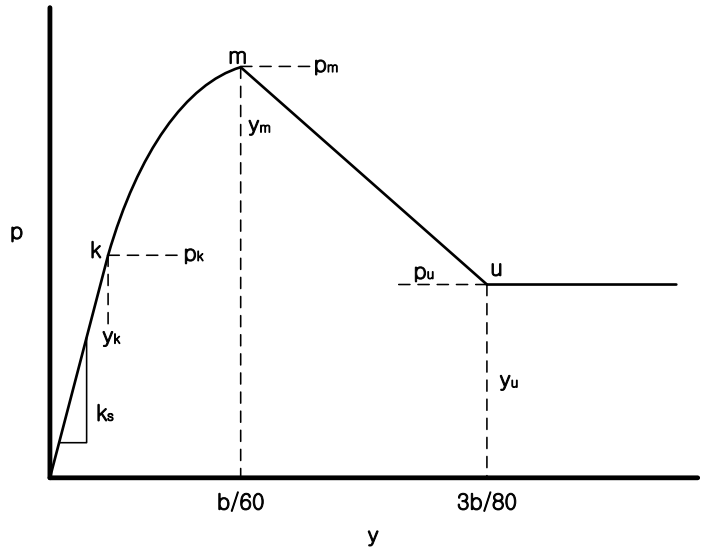

Figure 1.6.1 Soil response curve of soil retaining the components of both cohesion and friction angle

On the basis of the above facts, Evans and Duncan (1982) proposed an equation to approximately calculate the ultimate subgrade reaction for $c-\phi$ soils as follows:

$$p = \sigma_p b = C_p \sigma_h b \tag{1.6.1}$$

σ_p above represents passive earth pressure reflecting the 3-dimensional wedge effect on the passive side; b is the pile width; and C_p is a non-dimensional correction factor.

σ_h is the passive earth pressure based on the Rankine's theory and is expressed as,

$$\sigma_h = \gamma x \tan^2\left(45 + \frac{\phi}{2}\right) + 2c\tan\left(45 + \frac{\phi}{2}\right) \tag{1.6.2}$$

γ is the unit weight of soil; x is the depth at which passive resistance is considered; ϕ is the internal friction angle of soil; and c is cohesion.

The non-dimensional correction factor, C_p can be divided into the cohesion term and the internal friction angle term. By representing the cohesion term by C_{pc} and the internal friction angle term by $C_{p\phi}$, the equation below can be expressed.

$$p_u = \left[C_{p\phi}\gamma x \tan^2\left(45 + \frac{\phi}{2}\right) + C_{pc}\tan\left(45 + \frac{\phi}{2}\right)\right] b \tag{1.6.3}$$

Based on the concept suggested by Evans and Duncan (1982), the p-y curve for $c-\phi$ soil can be simply arranged as,

$$p_u = \overline{A} p_{u\phi} + p_{uc} \tag{1.6.4}$$

$\overline{A}$ is calculated from Figure 1.6.2. The ultimate subgrade reaction ($p_{u\phi}$) in the friction angle term is determined by the lesser of the following two expressions:

$$\begin{aligned} p_{u\phi} = \gamma x \Bigg[& \frac{K_0 x \tan\phi \sin\beta}{\tan(\beta-\phi)\cos\alpha} + \frac{\tan\beta}{\tan(\beta-\phi)}\left(b + x\tan\beta\tan\alpha\right) \\ & + K_0 x \tan\beta\left(\tan\phi\sin\beta - \tan\alpha\right) - K_a b \Bigg] \end{aligned} \tag{1.6.5}$$

$$p_{u\phi} = K_a b\gamma x\left(\tan^8\beta - 1\right) + K_0 b\gamma x \tan\phi \tan^4\beta \tag{1.6.6}$$

The ultimate subgrade reaction (p_{uc}) in the cohesion term is determined by the lesser of the following two expressions:

$$p_{uc} = \left[3 + \frac{\gamma'}{c}x + \frac{J}{b}x\right] cb \tag{1.6.7}$$

$$p_{uc} = 9cb \tag{1.6.8}$$

As the stress-strain relationship curve for $c-\phi$ soil is similar to that of sandy soil rather than cohesive soil, the calculation procedure suggested by Reese et al. (1974) is used.

① Determine p_u at $y_u = \frac{3b}{80}$ as follows:

$$p_u = \overline{A}_s p_{u\phi} + p_{uc} \tag{1.6.9}$$

$$p_u = \overline{A}_c p_{u\phi} + p_{uc} \tag{1.6.10}$$

Appropriate values of $\overline{A}_s$ and $\overline{A}_c$ are selected from static or cyclic loading on the basis of non-dimensional depth as shown in Figure 1.4.2.

② Determine p_m at $y_m = \dfrac{b}{60}$ as follows:

$$p_m = B_s p_s \ , \quad p_m = B_s p_s \tag{1.6.11}$$

Appropriate values of $\overline{B}_s$ and $\overline{B}_c$ are selected from static or cyclic loading on the basis of non-dimensional depth as shown in Figure 1.4.3.

As shown in Figure 1.6.1, the soil response curve is a straight line between $y_m = \dfrac{b}{60}$ and $y_u = \dfrac{3b}{80}$, and this straight line can be determined after calculating p_m and p_u.

③ The initial straight line part of the soil response curve is determined by,

$$p = (kx)y \tag{1.6.12}$$

k above is divided into the friction angle term and cohesion term and is expressed as,

$$k = k_c + k_\phi \tag{1.6.13}$$

And k_c and k_ϕ are determined from Figure 1.6.2.

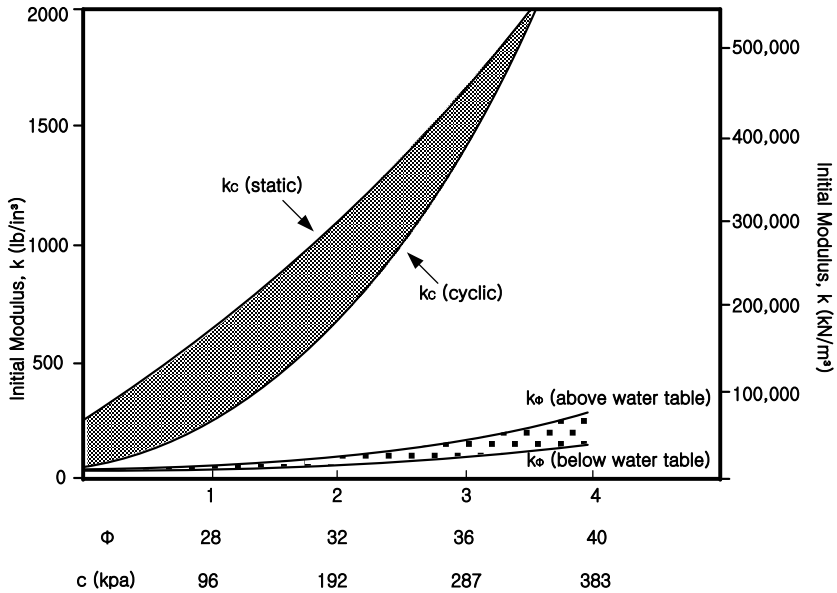

Figure 1.6.2 Typical k values for silt

④ Determine the parabolic part of the p-y curve from,

$$p = \overline{C} y^{1/n} \tag{1.6.14}$$

The curve between k and m is defined by the following procedures:

a. Determine the slope between m and u .

$$m = \frac{p_u - p_m}{y_u - y_m} \tag{1.6.15}$$

b. Determine the degree of the equation in the curve part.

$$n = \frac{p_m}{m y_m} \tag{1.6.16}$$

c. Determine the coefficient $\overline{C}$.

$$\overline{C} = \frac{p_m}{y_m^{1/n}} \tag{1.6.17}$$

d. Determine the displacement at point k.

$$y_k = \left(\frac{\overline{C}}{kx}\right)^{\frac{n}{n-1}} \tag{1.6.18}$$

If an intersection point exists between the straight line part and the curve part, the p-y curve is defined as shown in Figure 1.6.1. If no intersection point exists, an intersection with a subsequent curve is sought. If no intersection point exists with the subsequent equation, the initial straight line equation defines the entire p-y curve.

1.7 Ground Response Curve for Rock

Rock is regarded as foundation ground that supports major superstructures or large structures. By and large, piles cannot be driven into rock, but rather the ground is bored and piles are placed. Therefore, the ground response curve of rock differs from those of cohesive soil or sandy soil.

Rock is classified into hard rock and week rock according to the strength. The strength of rock is evaluated by R. M. R. (Rock Mass Rating) or R. Q. D. (Rock Quality Designation). In SoilWorks, R.Q.D. is used.

The ground response curve, which is used to analyze the pile behavior in rock, includes many uncertain elements. The aspects that can characterize rock such as rock types, joint properties, etc. are not reflected in the ground response curve. Therefore, subjective engineering judgment is required to realistically evaluate rock.

In addition, since the displacement of a pile in rock is infinitesimal, the ultimate resistance of rock cannot be measured from in-situ load tests. Nevertheless, when a lateral load is applied, it is necessary to estimate the ultimate ground resistance so as to find out the failure behavior of a pile.

1.7.1 Soil Response Curve for Hard Rock

Figure 1.7.1 shows the p-y curve under the action of lateral loading. As the parameters to define a p-y curve for rock are quite insufficient, the curve cannot reflect the increase in strength with depth. In addition, cyclic loading effects cannot be accounted for either.

As shown in Figure 1.7.1, when the lateral displacement of a pile exceeds $0.0004b$, brittle failure occurs. However, since experimental data is very limited in cases of rock, the engineer's discretion is required. In the field, rock behaves according to joints, cracks, etc., not based on the strength of a specimen.

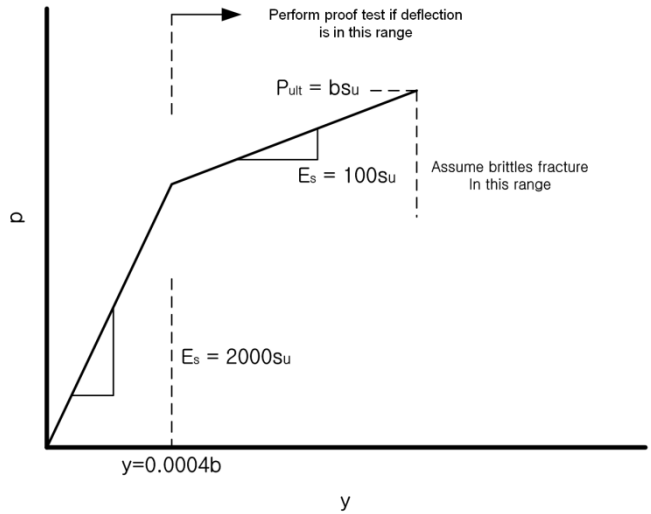

Figure 1.7.1 Ground reponse curve for hard rock

1.7.2 Ground Response Curve for Weak Rock

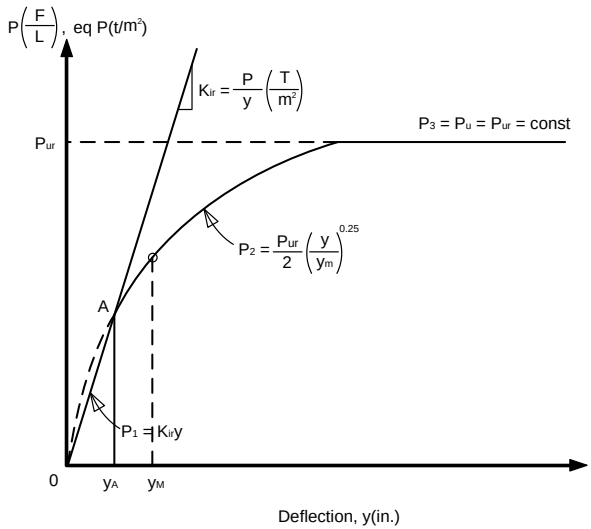

Figure 1.7.2 Ground response curve for weak rock

The ground response curve for weak rock is similar to that of sandy soil. The ultimate subgrade reaction of weak rock is determined with the assumption that wedge failure occurs in rock as follows:

$$p_{ur} = \alpha_r q_{ur} b \left(1 + 1.4\frac{x_r}{b}\right), \quad \left(0 \le x_r \le 3b\right) \tag{1.7.1}$$

$$p_{ur} = 5.2\alpha_r q_{ur} b, \quad \left(x_r > 3b\right) \tag{1.7.2}$$

q_{ur} is the uniaxial compressive strength of rock; α_r is a strength reduction factor; b is the pile diameter; and x_r is the corresponding depth.

The ground response curve for weak rock is based on sand stone, and the uniaxial compressive strength of rock q_{ur} is the only criterion. For the basis of simply defining the ground as weak rock in case the uniaxial compressive strength $q_{ur} < 6.9MPa$, overall evaluation should be reflected for such a classification.

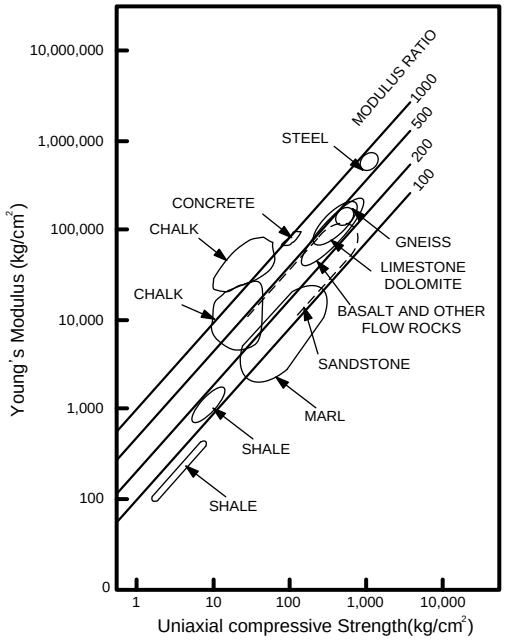

Figure 1.7.3 Ground deformation modulus of rock and uniaxial compressive strength

As rock can fracture even with small deformation, a strength reduction factor should be considered when the rock is evaluated by the uniaxial compressive strength alone. This is because a sound specimen is tested in a laboratory, whereas the ground is disturbed in the field due to the placement of piles. The strength reduction factor, α_r, which is used to estimate the behavior of a pile is defined as a function of RQD. In general, $\alpha_r = 1/3$ when RQD is 100, and $\alpha_r = 1$ when RQD is 0, the function of which is linearly increasing between the two factors.

In Figure 1.7.2, K_{ir} is determined from the following equation assuming that a beam is placed on a homogeneous elastic ground:

$$K_{ir} = k_{ir} E_{ir} \tag{1.7.3}$$

E_{ir} is the initial modulus of subgrade reaction of rock, and k_{ir} is the non-dimensional

coefficient.

The non-dimensional coefficient, k_{ir} is defined as,

$$k_{ir} = \left(100 + 400\frac{x_r}{3b}\right) \qquad 0 \le x_r \le 3b \tag{1.7.4}$$

$$k_{ir} = 500\,, \qquad x_r > 3b \tag{1.7.5}$$

$$p = K_{ir} y \qquad y \le y_A \tag{1.7.6}$$

$$p = \frac{p_{ur}}{2}\left(\frac{y}{y_m}\right)^{0.25} \qquad y > y_A\,, \quad p \le p_{ur} \tag{1.7.7}$$

$$p = p_{ur} \tag{1.7.8}$$

$$y_{rm} = k_{rm} b \tag{1.7.9}$$

where, the non-dimensional coefficient, $k_{rm} = 0.0005 \sim 0.00005$.

y_A is the intersection point between Eq. (1.7.6) and Eq. (1.7.7), which is given by,

$$y_A = \left(\frac{p_{ur}}{2 y_{rm}^{0.25} K_{ir}}\right)^{\frac{4}{3}} \tag{1.7.10}$$

The p-y curve for weak rock is determined based on the above equations.

In general, as rock itself has sufficient bearing capacity, there is no need to construct pile foundations. However, in case rock is significantly weathered and retains insufficient bearing capacity, cast-in-place piles are sometimes constructed. Even in such a case, the relevant equations are not based on sufficient data as outlined earlier, which calls for the engineer's judgment.

Chapter 2

Soil Response Curve for Axial Load

2.1 Overview

The load-displacement relationships due to lateral loads were reviewed in the previous chapter. In this chapter, the load-settlement relationships due to vertical loads will be studied. Load-settlement curves can be directly determined by axial load tests. In most cases, however, especially for preliminary design, such relationship curves are not necessary. In this chapter, predictions for load-settlement curves will be examined from the analytical point of view.

A typical load-settlement curve for deep foundation is shown in Figure 2.1.1. In the figure, the vertical dashed line to the right represents the load caused by plunging load. This load increases the pile settlement without any further increase in resistance. If the load increases to the point Q_p, the total settlement increases to the point P. If unloading takes place, the settlement follows the left line. Even after complete unloading, residual settlement remains.

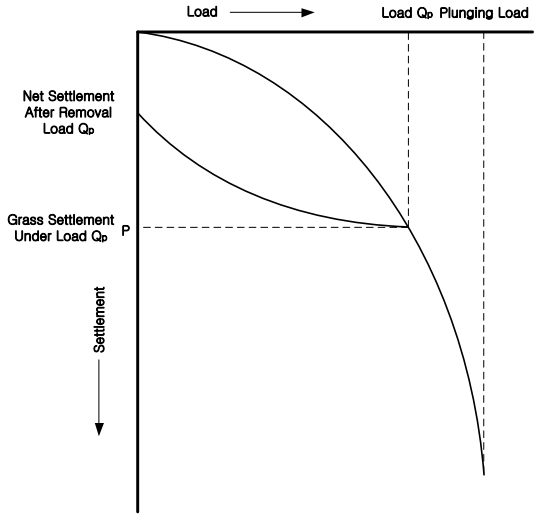

Figure 2.1.1 General axial load-settlement behavior

The load on a pile is transferred to soil as below. The axial load in a deep foundation is distributed along the length as shown in Figure 2.1.2. The slope represents the load distribution ratio.

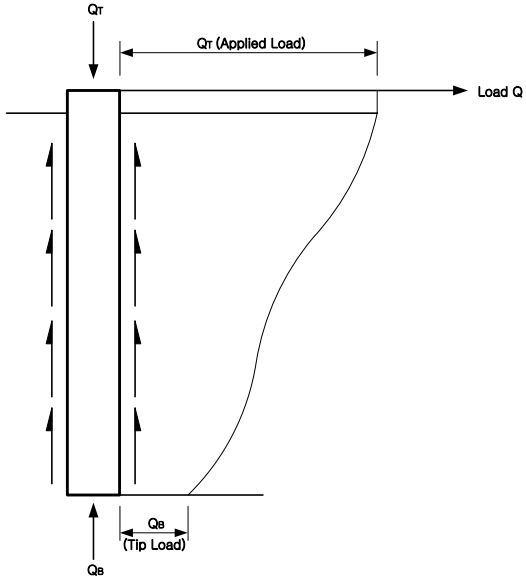

Figure 2.1.2 Load distribution over depth in a pile subjected to an axial load

There is no idealized model, which can define a deep foundation subjected to an axial load. In order to represent an actual pile, a few factors need to be combined as illustrated in Figure 2.1.3.

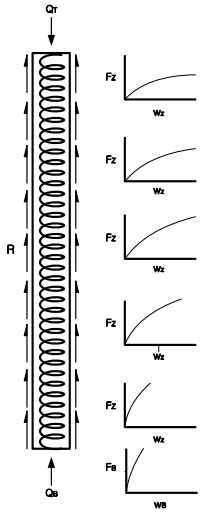

Figure 2.1.3 Soil behavior due to axial load

The spring elements shown in Figure 2.1.3 are a simplification of the real structural system. When Q_T is loaded on the pile, Q_B at the pile tip and R on the friction surface resist in equilibrium. Nonlinear springs are used not only along the length direction, but also on the pile tip.

In order to analyze the pile behavior, nonlinear equations need to be solved along the length direction of the pile for the given load.

2.2 Load Transfer Curve for Frictional Resistance in Cohesive Soil

Coyle and Reese (1966) proposed load transfer curves through conducting field and laboratory tests. The curves were obtained from full scale tests. The calculated results and the test results were relatively in good agreement as shown in Table 2.2.1.

Table 2.2.1 Load transfer due to settlement in cohesive soil

Load transfer / Maximum load transfer	Pile settlement (in)
0	0
0.18	0.01
0.38	0.02
0.79	0.04
0.97	0.06
1.00	0.08
0.97	0.12
0.93	0.16
0.93	0.20
0.93	0.20

Reese and O'Neill (1987) conducted numerous field tests and presented a developed load transfer curve as shown in Figure 2.2.1. The maximum load transfer took place at about 0.6% of the pile diameter. The pile diameters used in the tests ranged from $24in$ to $36in$, and the settlement at the total load transfer was about $0.2in$. Beyond the range, the equation by Coyle and Reese should be used.

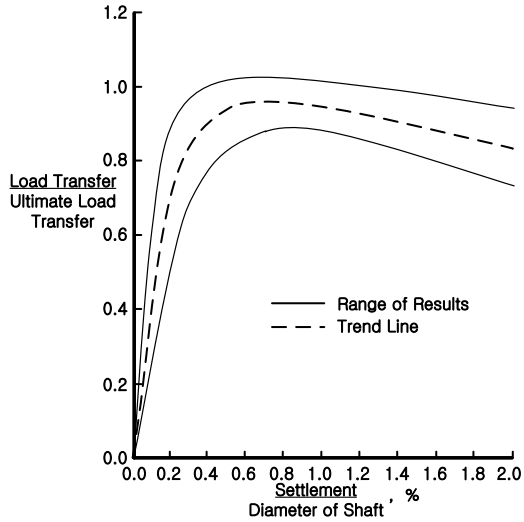

Figure 2.2.1 Non-dimensional load-settlement curve in cohesive soil (Reese and O'Neill, 1987)

2.3 Load Transfer Curve at Pile Tip in Cohesive Soil

Skempton (1951) conducted laboratory tests on stress-strain relationships for cohesive soil and presented the load-displacement relationships of pile tips. The strains (ε_{50}) at 50% of the ultimate compressive loads were within the limits between 0.005 and 0.02. The expression is written as,

$$q_b = N_c \left(\frac{\sigma_f}{2} \right) \tag{2.3.1}$$

$$\frac{w_b}{B} = 2\varepsilon_{50} \tag{2.3.2}$$

q_b above is the failure stress at the foundation; σ_f is the failure compressive stress; N_c is the bearing capacity factor; B is the foundation diameter; ε_{50} is the strain at an unconfined compressive state; and w_b is the settlement of foundation.

A stress-strain curve can be obtained from many tests, and the slope of the curve is about 0.5 on the logarithmic axis. If test data is unavailable, the slope of 0.5 can be used up to the failure stress.

The load-settlement curve of a pile tip is as follows:

$$Q_b = K_b \left(w_b \right)^n \tag{2.3.3}$$

where, K_b is an adjustment factor and n is normally 0.5.

Reese and O'Neill (1987) conducted a number of penetration pile tests in cohesive soil and presented the load-settlement curve as shown in Figure 2.3.1.

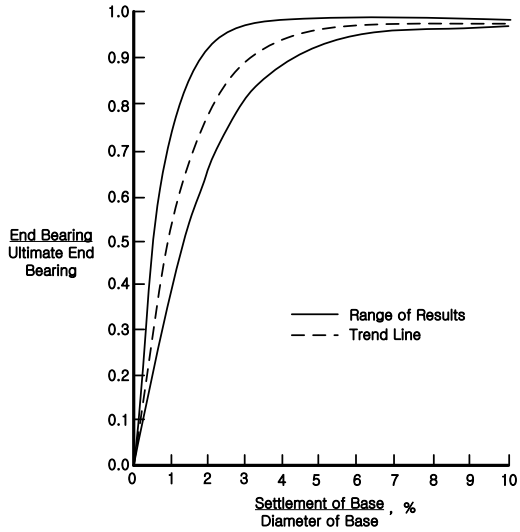

Figure 2.3.1 Non-dimensional load-settlement curve for pile tips in cohesive soil (Reese and O'Neill, 1987)

2.4 Load Transfer Curve for Frictional Resistance in Sandy Soil

Coyle and Sulaiman (1967) conducted load transfer tests for circumferential friction on steel piles in sandy soil and presented the results as shown in Figure 2.4.1.

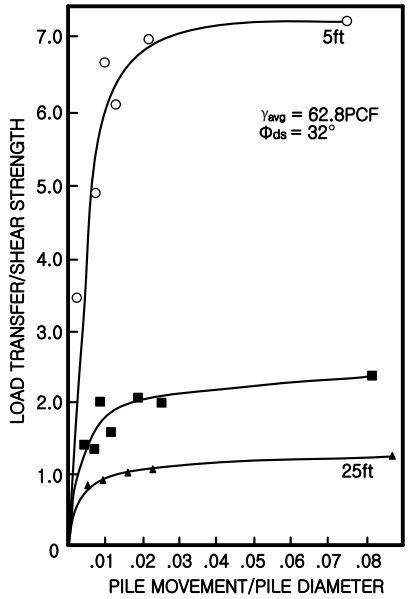

Figure 2.4.1 Load transfer curve in sandy soil (Coyle and Sulaiman, 1967)

The expression for the above curve is given by,

$$f = K_s \left(\frac{w}{B} \right)^{0.15}, \qquad \frac{Z}{B} \le 0.07 \tag{2.4.1}$$

f is the load transfer; w is the pile settlement; B is the pile diameter; and K_s is an adjustment factor.

Reese and O'neill (1987) conducted numerous full scale tests and calculated the load-

settlement curve in sandy soil as shown in Figure 2.4.2.

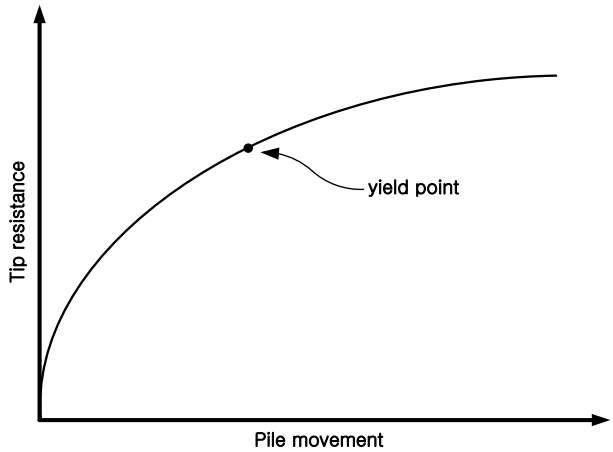

Figure 2.4.2 Displacement-resistance relationship at pile tip

Mosher (1984) calculated the load transfer curve for circumferential friction in sandy soil as follows:

$$f = \frac{w}{\frac{1}{E_s} + \frac{1}{f_{\max}} w} \tag{2.4.2}$$

where f is the unit load transfer; w is the pile settlement; $f_{\max}$ is the maximum unit load transfer; and E_s is a soil coefficient.

Table 2.4.1 Material properties for sandy soil

Relative density	Friction angle (ϕ)	$E_s \left(lbs / ft^2 / in\right)$
Loose	28-31	6,000-10,000
Medium	32-34	10,000-14,000
Dense	35-38	14,000-18,000

2.5 Load Transfer Curve at Pile Tip in Sandy Soil

Wijayvergiya (1977) and Mosher (1984) presented the following load-settlement curve for pile tips in sandy soil through a number of tests:

$$q = \left(\frac{z}{z_c} \right)^{1/3} q_{\max} \tag{2.5.1}$$

where the maximum bearing capacity ($q_{\max}$) is given by,

$$q_{\max} = \overline{\sigma_v} N_q \tag{2.5.2}$$

$\overline{\sigma_v}$ is the effective vertical stress, and N_q is a bearing capacity factor, which is calculated by the Meyerhof's equation as follows:

$$N_q = \varepsilon^{\pi \tan \phi} \tan^2 \left(45 + \frac{\phi}{2} \right) \tag{2.5.3}$$

Vijayvergiya (1977) correlated the limit displacement (z_c) to the width of a pile tip. If the displacement (z) is less than the limit displacement (z_c), the bearing capacity of the pile tip increases with displacement. When the displacement exceeds the limit displacement, the bearing capacity of the pile tip remains constant.

Mosher (1984) defined the maximum bearing capacity of a pile tip on the assumption that the pile tip behavior would be similar to that of an elasto-plastic material as shown in Figure 2.4.2. Mosher (1984) assumed that the pile would reach the state of yielding if the pile tip displacement exceeded $0.25in$.

$$q = \left(\frac{z}{0.25} \right)^{1/3} q_{\max} \tag{2.5.4}$$

This equation better coincides with the field measurement results, and the results for different densities are compiled as follows:

Loose $q = (4z)^{1/2} q_{\max}$

Medium $q = (4z)^{1/3} q_{\max}$

Dense $q = (4z)^{1/4} q_{\max}$

where the maximum yielding bearing capacity of a pile tip ($q_{\max}$) is determined by Eq. (2.5.2).

Chapter 3

Effects on Group Piles under Lateral Loads

3.1 Overview

Most tests performed in laboratories to obtain nonlinear p-y curves were conducted on single piles. However, piles are generally constructed in groups in practice. If the spacing of piles is too close, the lateral resistance of group piles is lower than that of individual piles collectively. In order to account for such reduction in capacity, Brown et al. (1987) introduced the f_m factor as shown in Figure 3.1.1.

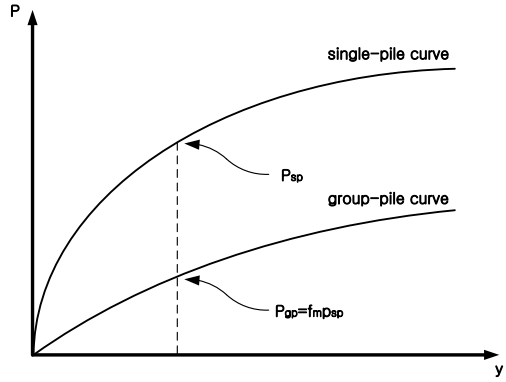

Figure 3.1.1 Definition of fm

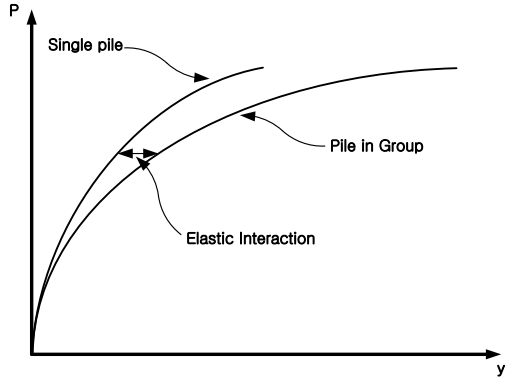

Figure 3.1.2 Group pile effects

When piles are spaced close enough to affect one another, the resistance is defined on the basis of the elastic theory as shown in Figure 3.1.2. In this case, the group piles retain the same ultimate resistance as a single pile.

In reality, the resistance of group piles is generally less than that of single piles. Thus, it is necessary to reduce the resistance according to the above-mentioned equation by Brown et al. (1987) as shown in Figure 3.1.3.

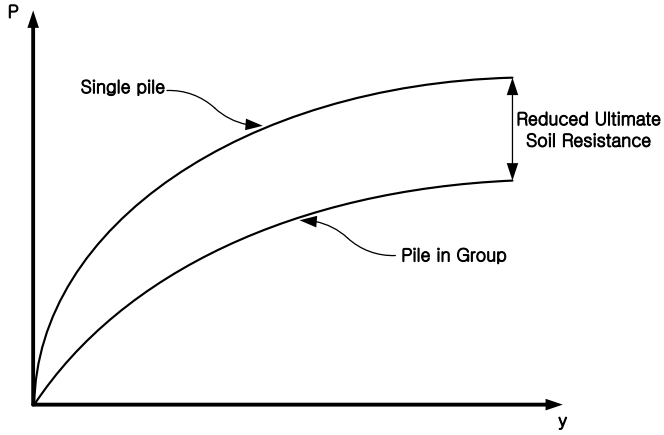

Figure 3.1.3 Reduction in resistance due to group pile effects

Among various reasons for the reduced resistance of group piles, SoilWorks considers only the effect of the spacing between piles. Chapter 3.2 and chapter 3.3 illustrate the ways of determining the reduction factors considering the transverse spacing and the longitudinal spacing between piles. Chapter 3.4 describes how to determine the reduction factor considering the diagonal spacing.

3.2 Reduction Factors for Loading in Transverse Direction

Prakash (1962), Cox et al. (1984), Wang (1986) and Lieng (1988) studied group piles of straight alignment subjected to lateral loads in the transverse direction in the fields. The reduction factor, β_a is expressed as a function of S/b (S is the center-to-center distance between the piles, and b is the pile diameter) as shown in Figure 3.2.1.

As shown in Figure 3.2.1, if the pile diameter is the same as the spacing, the ultimate resistance is reduced by 50%. If the spacing is greater than three times the diameter, no reduction in the ultimate resistance is observed. The reduction factor is irrelevant to the soil types.

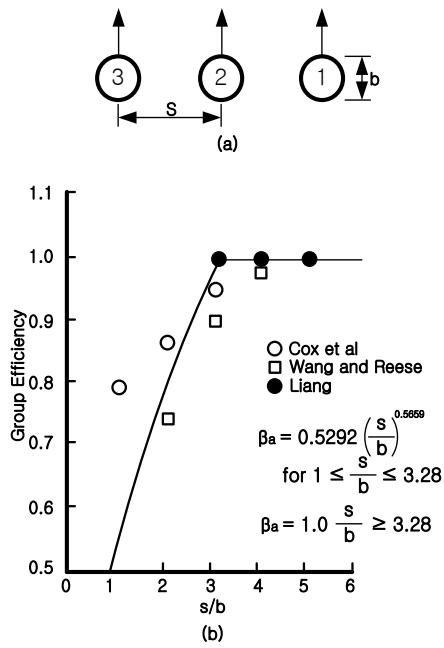

Figure 3.2.1 Resistance reduction factors for group piles subjected to transverse loading

3.3 Reduction Factors for Loading in Longitudinal Direction

When group piles are aligned in the direction of lateral loading, the pile-load interaction is more complex than the case of the transverse loading direction. Dunnavant and O'Neill (1986) investigated the behavior of longitudinal group piles considering the pile spacing and separating the preceding and succeeding piles. Like the transverse loading direction, soil properties were not considered in arriving at the reduction factors. Preceding piles in the longitudinal direction are illustrated in Figure 3.3.1b. In Figure 3.3.1a, Pile 1 precedes Pile 2 and Pile 3, and Pile 2 precedes Pile 3.

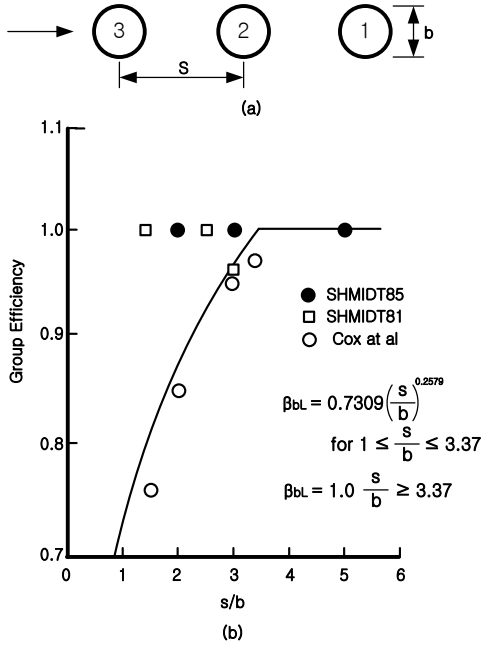

Figure 3.3.1 Reduction factors for preceding piles

The reduction factors for succeeding piles are shown in Figure 3.3.2b. In Figure 3.3.2a, Pile 3 succeeds Pile 1 and Pile 2, and Pile 2 succeeds Pile 1. As shown in Figure 3.3.2b, if s/b is greater than 6, the succeeding pile effects disappear.

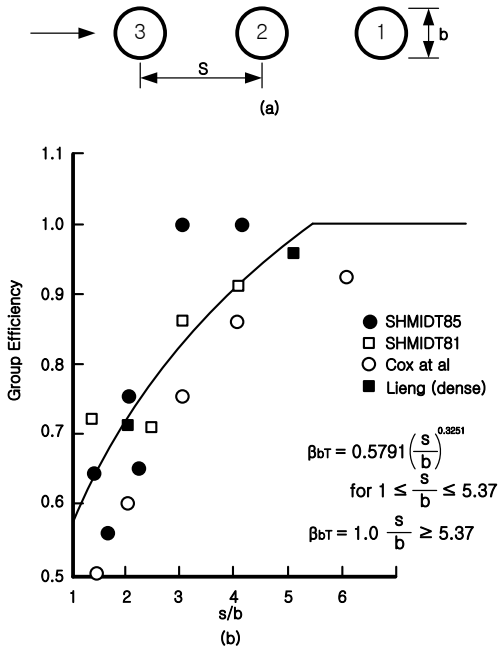

Figure 3.3.2 Reduction factors for succeeding piles

3.4 Reduction Factors for Diagonal Group Piles

It is difficult to find the reduction factors for diagonal piles empirically. Using an elliptical equation in the polar coordinate system, the reduction factors can be mathematically calculated in a simple manner. Figure 3.4.1 shows the correlation of group piles aligned diagonally to the direction of lateral loading. The lateral loding reduction factor, β_a can be determined by Figure 3.2.1, and the reduction factor, β_b can be determined by Figures 3.3.1 and 3.3.2 from which the reduction factor is given by,

$$\beta_s = \left(\beta_b{}^2 \cos^2\phi + \beta_a{}^2 \sin^2\phi\right)^{\frac{1}{2}} \tag{3.4.1}$$

where, ϕ is the angle between the loading direction and the line of piles.

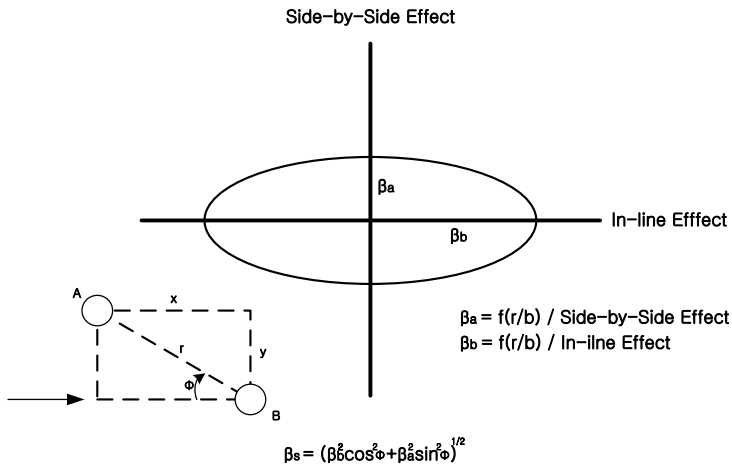

Figure 3.4.1 Reduction factors for diagonal piles